УДК 550.35:550.8.1 Doi: https://doi.org/10.32918/nrs.2020.3(87).04

Geospatial Modeling of Radon-Prone Areas

- **Dudar Tamara,** PhD (Geol. & Mineral.), Senior Research Scientist, Associate Professor
  National Aviation University, Kyiv, Ukraine
  ORCID: https://orcid.org/0000-0003-3114-9732

- **Titarenko Olga,** PhD (Engin.), Senior Research Scientist
  State Institution «Scientific Center for Aerospace Research of the Institute for Geological Sciences of NAS of Ukraine», Kyiv, Ukraine
  ORCID: https://orcid.org/0000-0001-5804-1022

- **Nekos Alla,** Dr. Sci. (Geogr.), Professor, Head of Chair
  V.N. Karazin Kharkiv National University, Kharkiv, Ukraine
  ORCID: https://orcid.org/0000-0003-1852-0234

- **Vysotska Olena,** Dr. Sci. (Engin.), Professor, Head of Chair
  National Aerospace University «Kharkiv Aviation Institute», Kharkiv, Ukraine
  ORCID: https://orcid.org/0000-0003-3723-9771

- **Porvan Andrii,** PhD (Engin.), Associate Professor
  National Aerospace University «Kharkiv Aviation Institute», Kharkiv, Ukraine
  ORCID: https://orcid.org/0000-0001-9727-0995

Methods for identification of potentially radon-prone areas using geospatial analysis in ArcGIS 10.6 software environment and mathematical modeling in SPSS 19.0 on the example of high background radiation area have been developed. High level of natural radioactivity associated with uranium content in environment objects and natural uranium occurrences, and also the spatial density of faults (reliable and unreliable) and lineaments were taken into account as well as the distance from uranium mine located nearby.

The method of linear discriminant functions was used to make a math model for determining the level of radon hazard. To do this, data on all locations were divided into training and test samples. Determination of predictors of the mathematical model was performed using Fisher's criterion by their sequential inclusion in discriminant equations. Among the considered 13 factors of radon hazard, seven of them turned out to be informative. For them, canonical coefficients were calculated using the least squares method for first- and second-order polynomials. Based on the values of discriminant functions, a territorial map was constructed to assign the new location to a certain level of radon hazard.

The maps obtained present the correlation of the radon-prone areas with the zones of high spatial density of faults and lineaments, and confirmed by the data of direct indoor radon measurements. In a limited number of measurements, the methods might get a good help in prioritization for round-the-country radon survey. As far as the model for identification of potentially radon-prone areas is mainly based on geological studies, the further research is supposed to be directed to its approbation for a different geological environment of the Ukrainian shield.

Keywords: radon-prone area, geospatial analysis, faults spatial density, spatial density of the 3-4 order lineaments, method of discriminant functions.

The concept of radon-prone areas («radon hazardous areas», «radon-affected areas») is considered in the context of Basic Safety Standards (BSS - EU Directive 59/2013, Article 103 §3). It is stated that a national action plan for public protection against radon should be developed and approved in each EU Member State and potentially hazardous areas have to be identified [1]. The EU BSS describes radon-prone areas as a geographic area where elevated indoor radon

SSTC NRS ДЕРЖАВНЕ ПІДПРИЄМСТВО ДЕРЖАВНИЙ НАУКОВО-ТЕХНІЧНИЙ ЦЕНТР З ЯДЕРНОЇ ТА РАДІАЦІЙНОЇ БЕЗПЕКИ

concentrations must be expected for natural reasons and surveys indicate that the percentage of households expected to exceed national reference levels is significantly higher than in other parts of the country. The European Atlas of Natural Radiation (EANR), a collection of maps displaying the levels of natural radioactivity from different sources [2], has not included any data on radon potential for Ukraine yet. At present, there is no national radon action plan. The strategy for public protection against the effects of radon exposure is under development, the methodology for identifying potentially hazardous areas at national level has not been developed yet and therefore these issues remain extremely relevant.

Analysis of previous studies

The issue of geogenic radon potential is widely covered in many European, especially Joint Research Center, publications [2] – [4]. Methodology for radon measurements and research of radon as a source of a significant human health risk is developed, in particular, by specialists from the State Institution «O.M. Marzieiev Institute for Public Health» of the National Academy of Medical Sciences of Ukraine and other experts [5] – [7]. Factors, which lead to formation of radon hazardous areas, are identified by ways of radon entry into the outdoor and indoor atmosphere and described in a wide range of publications, in particular in [8] – [12]. They all come down to the following natural reasons, which are supposed to get emphasized in the present research. The concentration of Rn-222 in the indoor air depends on the content of U-238 and/or Ra-226 in natural environment – rocks, weathering crust of parent material, soils and groundwater, on Rn-222 emanation coefficient from the soil, on the soil properties and condition, on concentration of uranium anomalies in the earth crust, and, consequently, on the concentration of uranium and radium in structural materials. Regarding the outdoor radon, its concentrations can be neglected.

Structural and tectonic geological factors play a significant role: deep-seated faults, fractured zones, zones of milonitization, brecciation, etc. Tectonic zones are considered as radon reservoirs where radon emanation coefficient is increased. When buildings are located above such zones, the likelihood of high concentrations of radon accumulating in them is abruptly increased. Apart from geological factors, buildings' materials and structures, ventilation, and behavior cultures are also considered [13] – [15]. However, our research is concentrated on the Central Ukrainian Uranium Province of the Ukrainian Shield and uranium mining area, and so we further focus mainly on geological factors.

Setting of research objectives

In [16], the territory of uranium mining and milling facilities legacy sites was outlined and classified (nine legacy sites altogether). The uranium mining has being developed here since the time after the Second World War. The sites of uranium mining (depleted through underground mining and in situ leaching and operating mines) were considered from their radiation hazard and remediation needs [17] – [18].

The presented research objective is to develop a methodology for the radon-prone area identification based on geospatial analysis and mathematical modeling.

Research materials and methods

The input data flow chart for geospatial modeling is presented in Figure 1. The data are borrowed from long-term geological research (1992-2003) archive materials [19] – [20], [26] - geological map of uranium and thorium mineralization of the Ukrainian Shield Precambrian formations of 1: 500 000, geological map of uranium and thorium mineralization of the Ukrainian Shield Ingulskyi megablock of 1:200 000, and also from uranium deposits and ore manifestations database [21] within the central part of the Ukrainian Shield. The map of Pre-Cenozoic deposits, neotectonic map, the soil map for the Kirovohrad district, as well as the relief surface data (SRTM, ALOS), and data on uranium content in different environment objects [20], [22]. Gamma activity of sedimentary rocks cover (μSv/h) [20] and dose rate at 1 m height (μSv/h) [10] were used as supplementary data. Altogether, 13 factors were taken into account (Table 1), and the score was appointed for each of factors so that they could be combined to obtain a comprehensive solution.

Therefore, first, a map of faults spatial density was made over a grid of 5 km x 5 km and analyzed in terms of association of high faults spatial density areas (dark brown colors) and ring structures for the territory outlined (Figure 2). Then, a research territory of the Kirovohrad uranium ore region was allocated for more thorough analysis at local level (40 km x 25 km). The research territory background data on the Michurinske ore field along with the Michurinske uranium deposit located at the intersection of the sub-longitudinal Kirovohrad tectonic zone and the Oleksandrivsko-Pervozvanskyi sub-latitudinal fault, as well as the vicinity of the Kropyvnytskyi city on the one hand, and the oldest Ingulska uranium mine on its south-eastern suburbs on the other hand, justified the choice of this area for research at local level.

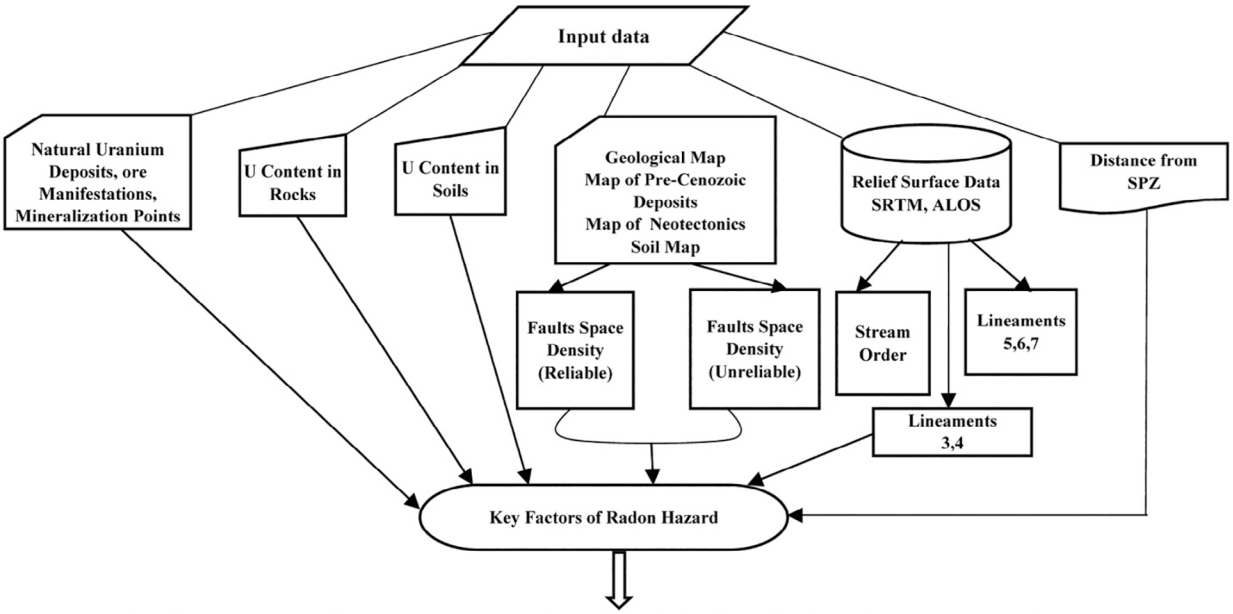

№	Natural Uranium Deposits, ore Manifestations, Mineralization Points	Uranium Content		Geological Data			Location
		U in Rocks, % 10^{-4}	U in Soils, % 10^{-4}	Reliable Faults	Unreliable Faults	Lineaments 3,4	Distance from SPZ
1	X1	X2	X3	X4	X5	X6	X7

Figure 1 – Input data flowchart for geospatial modeling

Table 1 – Radon hazard levels

A	B U deposits, ore manifestations		U content in							
			rocks $\cdot 10^{-4}$ %		weathering crust $\cdot 10^{-4}$ %		soils $\cdot 10^{-4}$ %		water $\cdot 10^{-6}$ g/L	
			C	C^1	D	D^1	E	E^1	F	F^1
1	not evident	1	5-6	1	0.06-0.07	1	0.5-0.9	1	3-6.4	1
2	mineralization	2	7-8	2	0.08-0.10	2	1.0-1.4	2	6.5-9.5	2
3	manifestations	3	9-10	3	0.11-0.12	3	1.5-1.9	3	9.6-12.8	3
4	ore deposits	4								

A	structural and geological								sedimentary cover				settlements			
	faults (reliable)		faults (unreliable)		lineaments				thickness of sedimentary cover, m		gamma dose rate of sedimentary cover μSv/h		distance from SPZ, m		dose rate at a height of 1 m, μSv/h	
					local 3-4		detail 6-7-8									
	G	G^1	H	H^1	I	I^1	I_1	I_1^1	J	J^1	K	K^1	L	L^1	M	M^1
1	0-0.124	1	0.11-0.26	1	0.2-0.43	1	0.6-1.52	1	≥ 50	1	0,09-0,10	1	≥ 15	1	0.08-0.09	1
2	0.125-0.31	2	0.27-0.41	2	0.44-0.67	2	1.53-3.65	2	25-49	2	0,11-0,14	2	11-14	2	0.10-0.11	2
3	0.32-0.5	3	0.42-0.56	3	0.68-0.9	3	3.66-5.78	3	10-24	3	0,15-0,20	3	6-10	3	0.12-0.13	3
4	0.51-0.7	4	0.57-0.71	4	0.91-1.14	4	5.79-7.9	4	≤ 9	4	0,21-0,33	4	1-5	4	> 0.13	4

SSTC NRS ДЕРЖАВНЕ ПІДПРИЄМСТВО ДЕРЖАВНИЙ НАУКОВО-ТЕХНІЧНИЙ ЦЕНТР З ЯДЕРНОЇ ТА РАДІАЦІЙНОЇ БЕЗПЕКИ

Fragment of filled in Table 1

№№	level of P RH	Uranium deposits	U content							
			U in rocks, $\cdot 10^{-4}$ %		U in weathering crust, $\cdot 10^{-4}$ %		U in soils, $\cdot 10^{-4}$ %		U in water, $\cdot 10^{-6}$ g/L	
	A	B	C	C^1	D	D^1	E	E^1	F	F^1
1	1	1	5-6	1	0.06-0.07	1	1.0-1.4	2	3-6.4	1

№№	structural and geological								sedimentary cover				settlements			
	faults (reliable)		faults (unreliable)		lineaments				thickness of sedimentary cover m		gamma dose rate of sedimentary cover μSv/h		distance from SPZ, m		dose rate at a height of 1 m, μSv/h	
					local 3-4		detail 6-7-8									
1	G	G^1	H	H^1	I	I^1	I_1	I_1^1	J	J^1	K	K^1	L	L^1	M	M^1
	0.125-0.31	1	26.5-41	2	43,6-7,04	2	0.6-1.52	1	25-49	2	11-12	2	6-10	3	0.10-0.11	2

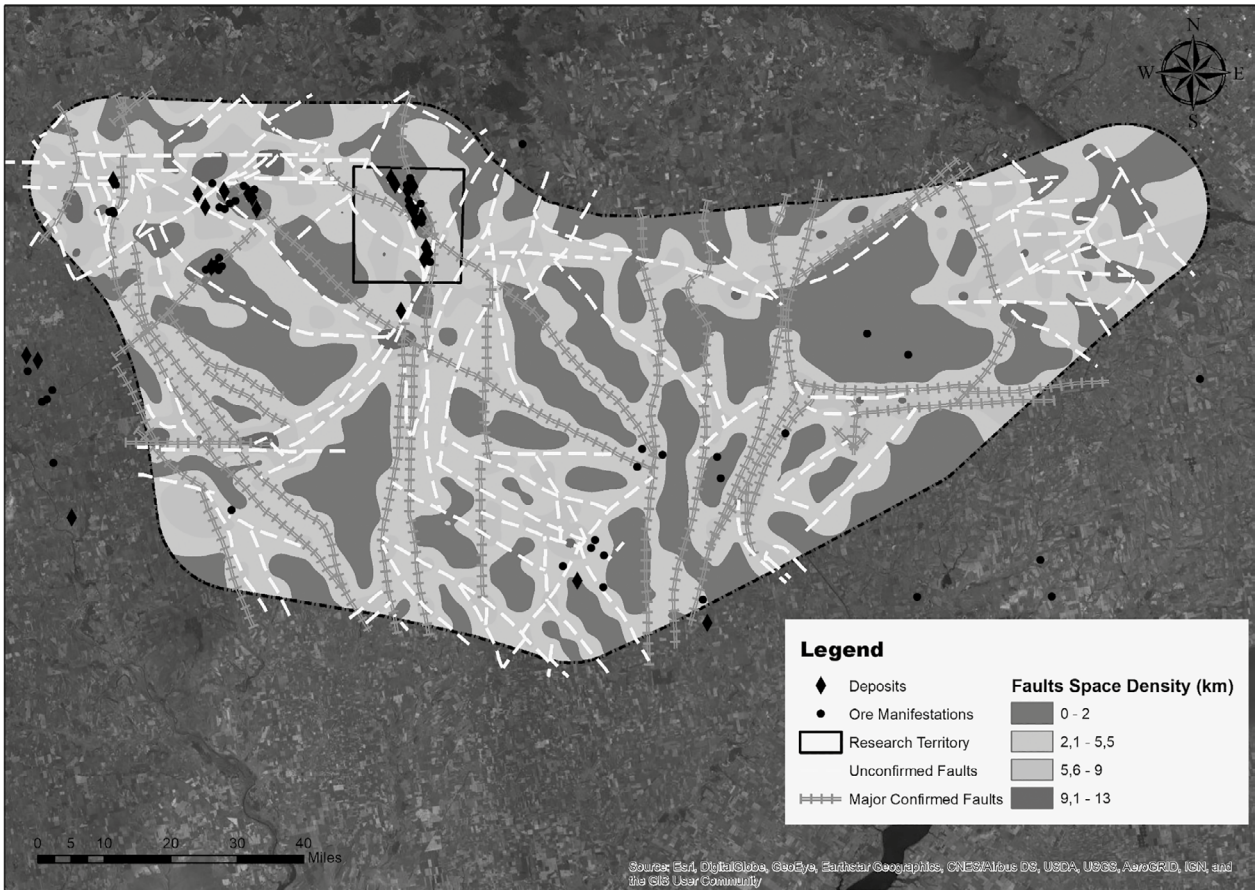

Figure 2 – Faults Spatial Density

Another map of faults spatial density and a map of spatial density of the 3-4 order lineaments (Figure 3) were made over a grid of 1 km x 1 km for the chosen local site in the ArcGIS 10.6 software environment Then, forty different locations were allocated and considered, so as to smoothly cover zones of different faults and lineaments spatial density (four levels) according to obtained maps. Each location was analyzed in terms of their characterization according to 16 previously proposed factors and database of 40 items was created in the form of a table with the head similar to Table 2.

Mathematical modeling for radon-prone area identification

The method of discriminant functions was used to develop a forecasting model for radon-prone area identification. It is widely applied in various fields of human activities, as well as the other methods of mathematical statistics [23] – [25]. For this purpose, data on all locations were divided into training and testing samples, which included 70 % and 30 % of all observations, respectively. Four levels of potential radon hazard (PRH) were conditionally identified: from the lowest (the 1st) where locations belong to the zone of the lowest spatial faults density to the highest (the 4th) level where locations are concentrated within zones of highest spatial faults and lineaments density.

Each sample included research of all locations, respectively referred to four groups. From a mathematical point of view, all groups were considered as a set of objects with qualitative, varying characteristics. Based on these characteristics, the group to which the object belongs was determined. The mathematical processing of the results was carried out in SPSS 19.0 software environment [26].

Three discriminant functions of the following type are needed to determine the group membership:

$$DF = b1 \cdot 1 + ... + bixi + \ldots + bpxp + C,$$

where DF is the discriminant function value; xi is the quantitative value of the i-th attribute; bi is the i-canonical coefficient of discriminant function (contribution of the i-th attribute to the function value); p is the number of attributes; C is the constant.

The mathematical model predictors were determined using the Fisher Statistics by their sequential inclusion in the discriminant equations. Seven of fifteen considered radon hazardous factors were turned to be informative, and canonical coefficients were calculated for them using the

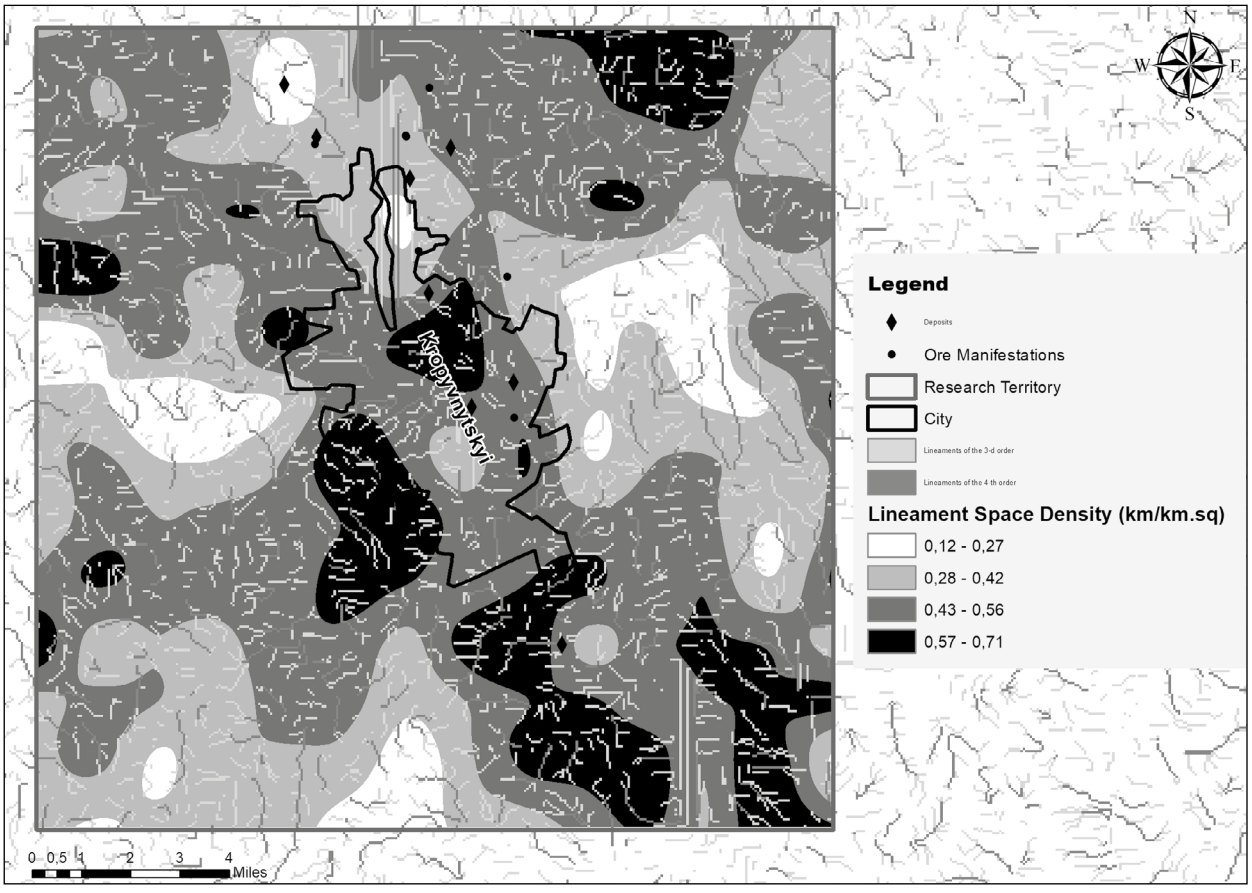

Figure 3 – Spatial Density of the 3-4 Order Lineaments

SSTC NRS ДЕРЖАВНЕ ПІДПРИЄМСТВО ДЕРЖАВНИЙ НАУКОВО-ТЕХНІЧНИЙ ЦЕНТР З ЯДЕРНОЇ ТА РАДІАЦІЙНОЇ БЕЗПЕКИ

least squares method for the first and second order polynomials. Determination of the mathematical model predictors and the canonical coefficients of the discriminant functions are presented in Table 2.

Therefore, the radon-prone areas identification can be described by the following discriminant functions:

$DF1(X)=0.532\cdot X1+1.746\cdot X2+1.485\cdot X3+$
$+0.851\cdot X4+0.153\cdot X5+0.900\cdot X6+0.474\cdot X7-14.871,$

$DF2(X)=1.588\cdot X1+0.047\cdot X2+1.352\cdot X3-$
$-1.338\cdot X4-0.845\cdot X5-1.258\cdot X6+0.997\cdot X7-2.208,$

$DF3(X)=-0.053\cdot X1+1.398\cdot X2-0.982\cdot X3+$
$+0.195\cdot X4-0.983\cdot X5+0.776\cdot X6+0.776\cdot X7-2.934.$

Based on the discriminant function values, a territorial map of a new object classification was developed (Figure 4). The territorial map defines the distribution in the area that determines the group affiliation (Table 3). However, within the relevant area, the likelihood of being in this group is higher than for the other groups [27]. Within the areas, the probability for boundary groups is the same.

Table 2 – Coefficients of canonical discriminant function

Model's predictors	Function		
	1	2	3
X_1 – Uranium Deposits and Ore Manifestations	0.532	1.588	-0.053
X_2 – Uranium Content in Rocks	1.746	0.047	1.398
X_3 – Uranium Content in Soils	1.485	1.352	-0.982
X_4 – Reliable Faults Spatial Density	0.851	-1.338	0.195
X_5 – Unreliable Faults Spatial Density	0.153	-0.845	-0.983
X_6 – Local Lineaments Spatial Density	0.900	-1.258	0.767
X_7 – Distance from Sanitary Protection Zone	0.474	0.997	0.776
Constant	-14.871	-2.208	-2.934

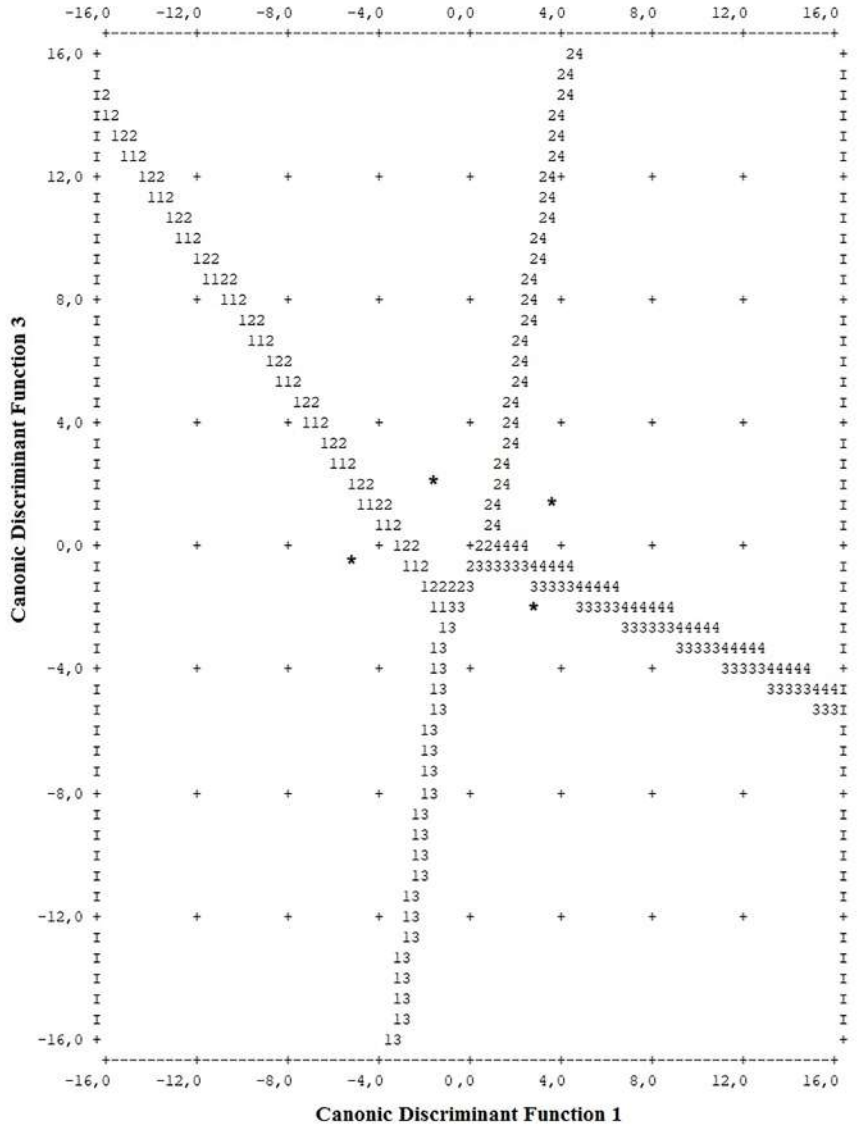

Figure 4 – Territorial map of object classification

Table 3 – Symbols used in the territorial map

Symbol	Group	Level
1	1	first (lowest) level of PRH
2	2	second level of PRH
3	3	third level of PRH
4	4	forth (highest) level of PRH
* Indicates a group centroid		

The correlation coefficients between calculated values of discriminant functions and indicators of group affiliation served a good measure for distribution into groups (Table 4). The obtained eigenvalues are provided in descending order of their values. The value of the eigenvalue is associated with the discriminant capabilities of the function: the higher the eigenvalue, the better the difference. A qualitative estimate of the r_{xy} link density was established based on the Cheddock scale.

Table 4 – Eigenvalues of the correlations of discriminant functions

Function	Eigenvalue	% Variance	Canonical Correlation r_{xy}
1	14,713	80,9	0,968
2	3,225	17,7	0,874
3	0,243	1,3	0,442

Additionally, the Wilks' Lambda test was conducted to determine whether the average values of discriminant functions in groups significantly differ among themselves (Table 5).

Table 5 – Results of Wilks' Lambda test

Test of Function(s)	Wilks' Lambda	Significance p
1 to 3	0,012	0,001
2 to 3	0,490	0,070
3	0,804	0,200

The obtained discriminant functions allow correct classification of the four groups according to seven predictors. The classification results for the training sample are presented in Table 6.

Results and discussions

Large-scale studies conducted in Western Europe in the early 1990s have shown that radon produces between 50 % of the collective dose for radon-safe areas and up to 92 % for regions of high radon potential. In the mid-1990s, the State Enterprise «Kirovheolohiia» and other Research Institutions of Ukraine performed radioecological studies on radon in residential areas of the city of Kropyvnytskyi (Kirovohrad) and in the Kirovohrad district [10]. It was determined that 50 % of the surveyed neighborhoods belong to radon-prone areas, including 33.7 % - where indoor radon exceeds 100 Bq/m^3, 11,4 % - 200 Bq/m^3, 0,14 % - 1000 Bq/m^3. In general, it was determined that the number of houses, in which the average annual radon equilibrium equivalent concentration exceeds 100 Bq/m^3 is 53 % of the total number of surveyed houses [10, Kirovheolohiia Archive Materials, 1992-1996].

The research of radon hazard for the Kirovohrad uranium ore region shows the association of the most radon hazardous areas directly with zones of high spatial density of faults and 3-4 order lineaments that is confirmed by high indoor radon values in the neighborhoods of the Kropyvnytskyi city (Figure 5).

Table 6 – Classification results of training sample objects

Level of Potential Radon Hazard PRH		Assumptive Group Membership				Total
		first (lowest) level of PRH	second level of PRH	third level of PRH	forth (highest) level of PRH	
Original, %	first (lowest) level of PRH	10	0	0	0	10
	second level of PRH	0	9	0	0	9
	third level of PRH	0	0	9	1	10
	forth (highest) level of PRH (potentially radon-prone areas)	0	0	0	11	11

SSTC NRS ДЕРЖАВНЕ ПІДПРИЄМСТВО ДЕРЖАВНИЙ НАУКОВО-ТЕХНІЧНИЙ ЦЕНТР З ЯДЕРНОЇ ТА РАДІАЦІЙНОЇ БЕЗПЕКИ

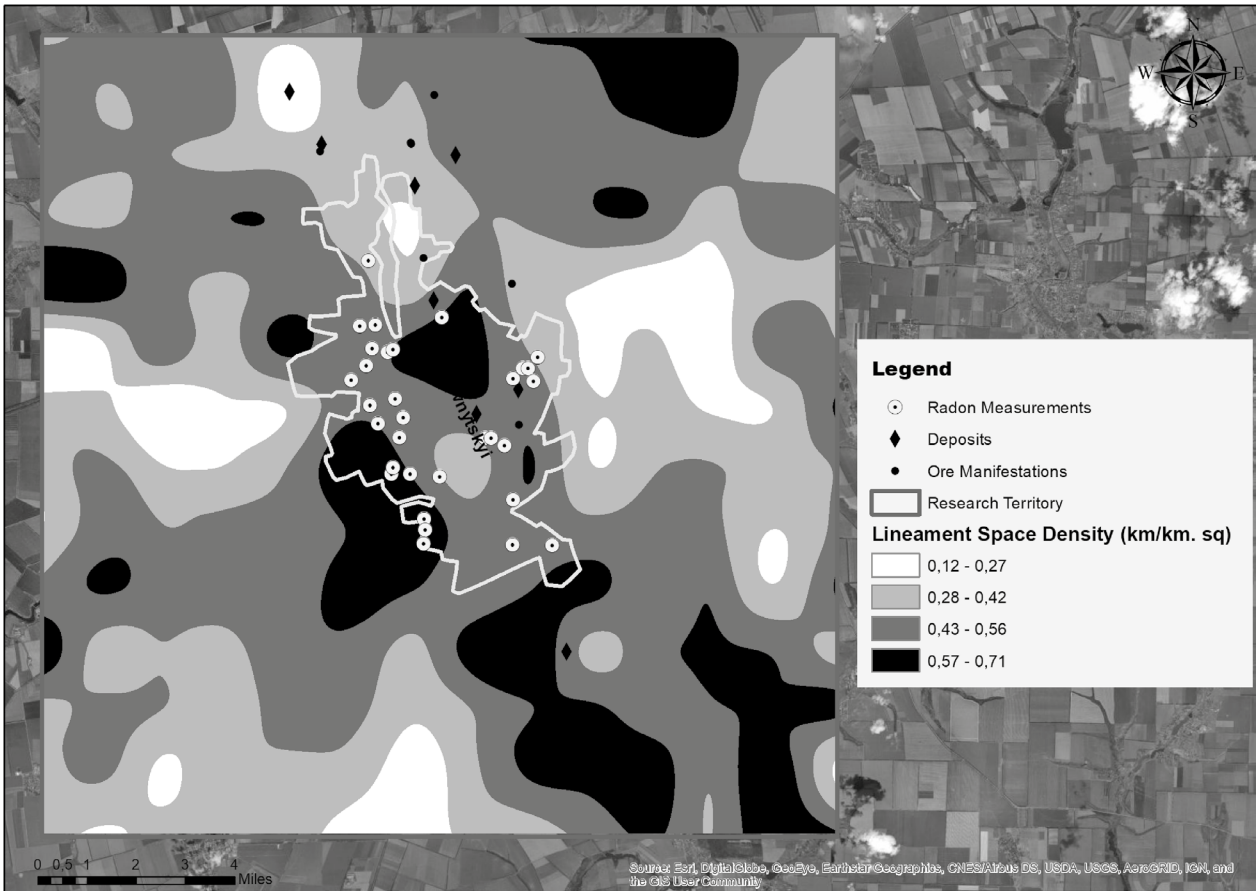

Figure 5 – Spatial density of 3-4 orders lineament and indoor radon measurements

Our studies have shown interesting results regarding the joint use of geospatial analysis and mathematical forecasting for zoning of the territory by the radon hazard level in the ArcGIS 10.6 software environment. Spatial faults (reliable and unreliable) density and then spatial density of the 3-4 order lineaments were taken first into consideration as the basic parameters for the initial stage of radon mapping at regional level. Other parameters were added further for a more detailed characterization of the radon hazardous area depending on the chosen location under consideration at local level. The presented technique can be applied to any territories where there is a high level of geological exploration, which allows development of a database of radon hazard factors.

It should be noted that our research confirms that the obtained high indoor radon concentrations are located within the radon-prone areas determined based on geospatial analysis, including the city of Kropyvnytskyi.

Analysis of the mathematical model classification results showed that all objects of groups 1, 2 and 4 were correctly classified. When classifying objects of the group 3, only 90 % of cases were correctly identified and 10 % were assigned to another group. Thus, the accuracy of potential radon hazard level was 97.5 % based on the training sample data.

Analyzing the obtained eigenvalues of the first and the third discriminant functions, equaled to 14,713 and 0,243, one can make a conclusion that the classification capabilities of the first discriminant function are almost 61 times greater than the third one.

When estimating the values of the canonical correlation coefficients, amounted to 0.968 and 0.442, respectively, of the first and third discriminant functions, it is possible to conclude that there is fairly high connection between the radon hazard level and the value of the first discriminant function, which is confirmed by the percentage of this function dispersion – 80.9 %.

During the Wilks' Lambda test, a very significant result was found between the first and third functions ($p < 0.001$) and a non-significant result between the last functions. Accordingly, it can be concluded that to identify the radon hazard areas, it is sufficient to use the first DF_1 and the third DF_3 discriminant functions.

When testing the developed mathematical model in the test sample, it was found that the prediction was made correctly for all four groups (Table 7).

Thus, the overall percentage of correct prediction of the radon-prone areas can make up 98.2 %, if the

Table 7 – Classification of the test sample objects

Level of Potential Radon Hazard PRH		Predicted Group Membership, %				Total
		first (lowest) level of PRH	second level of PRH	third level of PRH	forth (highest) level of PRH	
Original, %	first (lowest) level of PRH	100	0	0	0	100
	second level of PRH	0	100	0	0	100
	third level of PRH	0	0	100	0	100
	forth (highest) level of PRH *(potentially radon-prone areas)*	0	0	0	100	100

data of the new classification object are identical to the statistical distribution of the data that were the basis for the mathematical model development.

Thus, the overall rate of correct prediction of the level of potential radon hazard of the territory can be 98.2 %, if the criteria for the selection of a new object of study will be identical to the statistical distribution of data that formed the basis for a mathematical model development. For practical use of the model, it is supposed to determine the degree of conformity of the calculated model to the new object of research. It determines the prioritization or replacement of radon hazard factors (among the proposed 13), or addition of new significant factors, the importance of local characteristics of areas for radon hazard studies, that will require adapting the model and establishing adequacy to the new object.

Conclusions

1 In the context of the EU Basic Safety Standards, where radon-prone areas are required to be identified, it is proposed to use remote sensing methods for geospatial modeling of radon-prone areas, first at regional and then at local levels. The basic parameters for the initial mapping stage are supposed to be the faults and the lineaments of the 3rd and 4th level spatial density. Other parameters are added for more detailed analysis, depending on the particular location under consideration.

2 A mathematical model for the level of radon potential identification was developed based on the method of linear discriminant functions. High level of natural radioactivity associated with uranium content in environment objects and natural uranium occurrences, and also the spatial density of faults (reliable and unreliable) and lineaments were taken into account as well as the distance from uranium mine located nearby. The model developed allows classifying the level of radon potential in 98.2 % correctly.

3 As far as in European countries the indoor radon measurements are accepted on unified requirements and on a grid of 10 x 10 km, for countries intending to join the EU radon program, such measurements may be impossible due to various, primarily economic reasons. In a limited number of direct indoor radon measurements, remote methods are supposed to be a good help in identification of potentially radon hazardous level. Therefore, the radon survey can be further prioritized based on potential level identified on geospatial and mathematical modeling data.

4 As far as our model for identification of potentially radon-prone areas is mainly based on geological studies, the further research is supposed to be directed to its approbation for a different geological environment of the Ukrainian shield, for example, the highly populated Kyiv oblast area.

References

1. EC Council Directive 2013/59/Euratom (2014). Laying down basic safety standards for protection against the dangers arising from exposure to ionising radiation. *Official J. Eur. Union*, 57(L13), 1–73.

2. Cinelli, G., Tollefsen, T., Bossew, P., Gruber, V., Bogucarskis, K., De Felice, L., De Cort, M. (2019). Digital version of the European Atlas of natural radiation. *J. Environ Radioact*, 196:240-252. doi: 10.1016/j.jenvrad.2018.02.008.

3. Szabó, K.Z., Jordan, G., Horváth, Á., Szabó, C. (2014). Mapping the geogenic radon potential: methodology and spatial analysis for central Hungary. *J. Environ. Radioact*, 129, pp. 107–120.

4. Garcia-Talavera, M., Garca-Perez, A., Rey, C., Ramos, L. (2013). Mapping radon-prone areas using γ-radiation dose rate and geological information. *J. Radiol. Prot.*, 33, pp. 605–620.

5. Pavlenko, T. A., Los, I. P., Aksenov, N. V. (1997). Exposure doses due to indoor Rn-222 in Ukraine and basic directions for their decrease. *Radiat. Meas.*, 28, pp. 733-738.

6. Pavlenko, T., German, O., Fruziuk, M., Aksenov, N., Operchyuk, A. (2014). The Ukrainian Pilot Project "Stop Radon". *Nuclear Technology&Radiation Protection*, 29(2), 1-7.

7. Molchanov, O., Soroka, Y., Buzinny, M., Pavlenko, T., Podrezov, A., Soroka, M. (2010). Dispersion of radon in the atmosphere around old uranium mill tailings. Nukleonika, 55(4), 535-538.

8. Orliuk, M. I., Marchenko, A. V., Yatsevskyi, P. I. (2018). Radon and geomagnetic anomalies in Ukraine. *Dopovidi NAS of Ukraine*, 5, pp. 60-66.

SSTC NRS ДЕРЖАВНЕ ПІДПРИЄМСТВО ДЕРЖАВНИЙ НАУКОВО-ТЕХНІЧНИЙ ЦЕНТР З ЯДЕРНОЇ ТА РАДІАЦІЙНОЇ БЕЗПЕКИ

9. Lebed, O. O. Myslinchuk, V. O., Andreev, O. A. (2017). Radon: monitoring and geoecological analysis of its impact on the ecosystem of the city of Rivne. Monograph, RMANUM, 208.

10. Kovalenko, G. D. (2013). Radioecology of Ukraine: Monograph. Kharkiv, INZEK, 344.

11. Titarenko, O. V. (2014). Operational assessment of geoecological state of Krivyi Rig city by remote sensing techniques. Dopovidi NASU, 9, pp. 74-78.

12. Verkhovtsev, V. G., Yuskiv, Yu. V. (2016). Surveying aspects of currently active geostructures of the Ukrainian Shield and its slopes. *Ukrainian Journal of Earth Remote Sensing*, 8, pp. 43–46.

13. Verkhovtsev, et al. (2014). Prospects for the development of uranium resource base of nuclear power of Ukraine. Kyiv, Naukova Dumka, 355.

14. Clavensjoe, B., Aakerblom, G. (2003). Radon book. Measures against radon in existing buildings. Stockholm, FORMAS, 131.

15. Fryziuk, M. A., Aksionov, N. V., Fedorenko, O. V., Slinchenko, V. A., Chuchupal, I. I. (2018). Estimation of the radon concentrations in children educational institutions of Kropyvnytskyi city for radon protective actions. *Environment and Health,* 3(88), 56-62.

16. Dudar, T. V. (2019). Uranium mining and milling facilities legacy sites: Ukraine case study. *Environmental Problems*, 4, pp. 212–218. doi: 10.23939/ep2019.04.212.

17. Dudar, T. V. Verkhovtsev, V. G. Lysychenko, G. V. Tyshchenko, Yu. Ye. (2018). Radon emanation as a source of radiation hazard to the environment. *Information & Security: An International Journal*. doi: 10.11610/isij.410x.

18. Dudar, T. V., Verkhovtsev, V. G., Tyshchenko, Yu. Ye., Kyselevych, L. S., Buglak O. V. (2019). Radon-prone areas: the Ukrainian Shield case study. XVIII[th] International conference "Geoinformatics: Theoretical and Applied Aspects", Kyiv, Ukraine.

19. Voinovskyi, A. S., Bochai, L. V., Nechaev, S. V. et. al. (2002). Comprehensive metallogenic map of Ukraine. Scale 1: 500,000. Explanatory note, Kyiv, UkrDGRI, State Geological Survey of the Ministry of Resources of Ukraine, 336.

20. Shumlyanskyi, V. O., Subbotin, A. G., Bakarzhiev, A. H. et. al. (2003).Technogenic contamination with radioactive elements in mineral ore deposits. Kyiv, Znannia Ukrainy, 113.

21. Mikhailichenko, O.M. (2018). Report on the Regional Geological Survey of the Territory of Ukraine "Mapping of the Uranium and Thorium Ore Manifestations of the Ukrainian Shield 1: 500,000". State Enterprise 'Kirovheolohiia', 150.

22. Fomin, Yu. O., Demikhov, Yu. M., Verkhovtsev, V. G., Dudar, T. V. (2019). Forms of uranium trace elements in albitites of the Ukrainian Shield. *Geochemistry of Technogenesis*, Collection of research papers of IEG NAS of Ukraine, Kyiv, 2(30), 106-118.

23. Nosov, K., Zholtkevych, G., Georgiyants, M., Vysotska, O., Balym, Yu., Porvan A. (2017). Development of the descriptive binary model and its application for identification of clumps of toxic cyanobacteria. *Eastern-European Journal of Enterprise Technologies*, 4(88), 4-11. doi: 10.15587/1729-4061.2017.108285.

24. Nekos, A., Shulika, B., Porvan, A., Vysotska, O., Zhemerov, O. (2017). Control over grape yield in the north-eastern region of Ukraine using mathematical modeling. *Eastern-European Journal of Enterprise Technologies,* 3(86), 51-59. doi: 10.15587/1729-4061.2017.97969.

25. Vysotska, O., Georgiyants, M., Nosov, K. et. al. (2018). Development of a spatial dynamical model of the structure of clumps of toxic cyanobacteria for biosafty. *Eastern-European Journal of Enterprise Technologies*, 10(96), 64-75. doi: 10.15587/1729-4061.2018.150273.

26. Marija J. Norušis (2011). IBM SPSS Statistics 19 Guide to Data Analysis. Pearson Prentice Hall, 651.

27. Balym, Y., Georgiyants, M., Vysotska, O., Pecherska, A., Porvan, A. (2017). Mathematical modeling of the colorimetric parameters for remote control over the state of natural bioplato. *Eastern-European Journal of Enterprise Technologies*. 10(88), 29-36. doi: 10.15587/1729-4061.2017.108415.

Геопросторове моделювання радононебезпечної території

Дудар Т. В. [1], **Тітаренко О. В.** [2], **Некос А. Н.** [3], **Висоцька О. В.** [4], **Порван А. П.**[4]

[1]Національний авіаційний університет, м. Київ, Україна
[2]Державна установа «Науковий центр аерокосмічних досліджень Землі Інституту геологічних наук Національної академії наук України, м. Київ, Україна
[3]Харківський національний університет імені В.Н. Каразіна, м. Харків, Україна
[4]Національний аерокосмічний університет ім М.Є. Жуковського «Харківський авіаційний інститут», м. Харків, Україна

Розроблено методику ідентифікації потенційно радононебезпечних територій з використанням геопросторового аналізу в програмному середовищі ArcGIS 10.6 та математичного моделювання в програмному середовищі SPSS 19.0 на прикладі території з високим рівнем природної радіоактивності. Основними параметрами для початкового етапу картування пропонується просторова щільність розломів та просторова щільність лінеаментів 3-4 порядків. Інші параметри додаються для більш детального аналізу, залежно від конкретної локації, що розглядається. Отримані карти показують позитивну кореляцію радононебезпечних ділянок із зонами високої просторової щільності розломів та лінеаментів та підтверджуються даними безпосередніх замірів радону в приміщеннях. За умови обмеженої кількості вимірювань, ця методика може бути корисною у визначенні пріоритетності для радонової зйомки по країні.

Ключові слова: геопросторовий аналіз, метод дискримінантних функцій, радононебезпечна територія, просторова щільність лінеаментів 3-4 порядку, просторова щільність розломів.

Отримано 13.04.2020.